

THE EFFECTS OF LANCE POSITIONING AND DESIGN ON THE CO-INJECTION OF PULVERIZED COAL AND NATURAL GAS INTO BLAST FURNACES

Adrian MAJESKI¹, Allan RUNSTEDTLER^{1*}, John D'ALESSIO², Neil MACFADYEN³ and Kyle FERRON²

¹ Natural Resources Canada, CanmetENERGY, 1 Haanel Drive, Ottawa, Ontario, K1A 1M1, CANADA

² U. S. Steel Canada Inc., 386 Wilcox Street, Hamilton, Ontario, L8N 3T1, CANADA

³ Union Gas Ltd., 50 Keil Drive North, Chatham, Ontario, N7M 5M1, CANADA

*Corresponding author, E-mail address: Allan.Runstedtler@nrcan.gc.ca

ABSTRACT

Optimizing the co-injection of pulverized coal and natural gas into blast furnaces helps reduce metallurgical coke requirements, providing a net decrease in the costs and CO₂ emissions associated with iron production. Ideally, the fuel would enter the raceway partially reacted and the injection would not have negative impacts on the equipment. Success in achieving this outcome is sensitive to the details of how the injection is implemented. Given this sensitivity, and the facts that it is difficult to make accurate, detailed observations in blast furnaces or devise representative pilot-scale experiments, computational fluid dynamics (CFD) has become a useful and complementary tool for the analysis and design of fuel injection methodologies. This CFD modeling study examines the interaction of the blast air and fuel flows in the blowpipe and tuyere nozzle. A key question for the industry is how much effort and cost should be spent on lance design versus the benefit expected. Important operating issues such as initiation of reactions and heat loads on the tuyere nozzle are examined for two coal dispersion strategies. It is found, unexpectedly, that a bluff body effect on the blast air is effective at dispersing coal, especially for the smaller particle sizes. Based on the results of this study, future designs will focus on a single lance injecting both natural gas and coal and employing a bluff body effect to disperse the coal.

NOMENCLATURE

A	reaction rate parameter
C_{stoich}	stoichiometric coefficient
E_a	activation energy
k	reaction rate constant
R	reaction rate
T	temperature
ε	turbulence kinetic energy dissipation rate
κ	turbulence kinetic energy
\mathfrak{R}	universal gas constant
[fuel]	concentration (<i>e.g.</i> , of fuel)

INTRODUCTION

In the basic operation of a blast furnace for iron-making, metallurgical coke, iron ore, and limestone flux are supplied through the top of the furnace while hot air is blown through tuyeres (nozzles) into the lower section. Additional improvement is now routinely achieved by

oxygen enrichment and hydrocarbon fuel injection in the hot blast air, enabling a reduction in metallurgical coke requirement and improved productivity of the furnace, which results in energy, emissions, and cost savings. One limit to the addition of hydrocarbon fuel is its global cooling effect on the furnace relative to the corresponding use of metallurgical coke. Hydrocarbon injection does, however, provide advantages by introducing hydrogen into the furnace. The presence of hydrogen reduces the pressure drop of gas flow through the coke/ore burden or, alternatively, the upward force opposing the burden descent, because hydrogen is a lighter gas. Hydrogen and water vapour also diffuse more rapidly in and out of the ore pellets than carbon monoxide and carbon dioxide because of their higher diffusivities.

The details of implementing hydrocarbon fuel injection are known to be challenging, in terms of achieving partial combustion and controlling heat loads on the tuyeres. The hot blast air, travelling at approximately 150 m/s, provides only 5-10 milliseconds for combustion reactions to initiate in the tuyere. On the other hand, partially combusting the hydrocarbon fuel results in local heat release, which can cause excessive wear on the tuyeres. The blast air, typically having a temperature of 1100°C and speed of 150 m/s, presents a harsh environment for observation and measurement and it is expensive to carry out a trial-and-error approach in real furnaces. On the other hand, the rationalization of laboratory measurements to obtain commercial-scale predictions presents significant uncertainty. Consequently, CFD modelling has been increasingly used, along with observational data—at both pilot and commercial scales—and traditional methods of analysis, to help understand and design injection strategies.

CFD studies have been carried out for blast furnace injection but detailed studies on the co-injection of coal and natural gas are sparse in the open literature. Shen et al. (2009a,b) studied coal combustion in the blowpipe, tuyere, and simplified raceway and validated the combustion model against measurements in a test rig. They found that coal burnout strongly depends on the availability of oxygen and that representation of the actual geometry is important. The lance had an annular design, with coal and nitrogen conveyed through the centre and a coolant—oxygen, air or methane—conveyed through the outer ring, all without swirl. Shen et al. (2011) then extended the model to include the raceway geometry and

the coke bed, using the same injection lance geometry. Andahazy et al. (2005) performed a CFD analysis to examine the differences between injection of oil and coke oven gas through a simple pipe lance for a commercial furnace. Yeh et al. (2012) performed CFD studies of pulverized coal and blast furnace top gas (BFG) injection and found that coal burnout decreased with increasing BFG injection because the BFG consumed oxygen. They also noted swirling of the blast air caused by the presence of the injection lances and its effect on mixing. Chui et al. (2003) developed a CFD model and compared its predictions to measurements from a pilot-scale reactor, supporting their modelling approach.

A few experimental studies have been carried out in laboratories and commercial furnaces, some accompanied by corresponding models. Mathieson et al. (2005) reviewed successive generations of combustion test rigs, each attempting to provide a closer approximation to the actual blast furnace. Test rig configuration was demonstrated to have a significant effect on coal burnout. An earlier laboratory study by Jamaluddin et al (1986) found that coal grind, devolatilization characteristics, and dispersion of the injected coal had significant effects on coal burnout. The difficulty of obtaining measurements in the lower part of a commercial blast furnace is apparent in the paper by Nogami et al. (2005). They reported measured temperatures in the coke bed but only to a maximum of 1200°C, at which point the thermocouples, which descended with the burden materials, melted.

The focus of this paper is to present a CFD study examining the co-injection of pulverized coal and natural gas, using separate lances for each fuel. The natural gas enters through a simple pipe and the coal enters through an annular pipe in which the coal is conveyed through the centre and an annular flow of cooling air is either swirled or turned off. Mixing, combustion, and heat loads to the tuyere are examined. The objective is to understand injection dynamics as they relate to key lance design concepts.

1. MODEL DESCRIPTION

1.1 Model Overview

The calculations were performed using the software platform ANSYS-CFX®. The gas flow field is described by a set of 3-D, steady state, Reynolds averaged, Navier-Stokes equations, closed by the standard $\kappa-\varepsilon$ turbulence model. They are solved for several gas species mass fractions. Particles of pulverized coal are modelled by Lagrangian tracking in which turbulent dispersion is included and full coupling of mass, momentum, and energy of particles with the gas phase is implemented. The Discrete Transfer radiation model is used with 16 rays and a composition-dependent absorption coefficient. Radiant exchange is included in the coal particle energy balance.

The model accounts for two heterogeneous coal reactions. Devolatilization is modelled according to an Arrhenius reaction rate with rate constant given by

$$k_{Devol} = (20,000 \text{ } \frac{1}{s}) e^{-\frac{5,000K}{T_{Particle}}} \quad (1)$$

where the pre-exponential and the activation energy are derived from the paper by Badzioch and Hawskley (1970) and the rate is zero below an onset temperature of 773 K. The char oxidation rate, in which $C + \frac{1}{2}O_2 \rightarrow CO$, is determined by a combination of O_2 diffusion to the particle surface and a chemical Arrhenius rate with rate constant given by

$$k_{Char} = (0.09962 \text{ } \frac{kg}{m^2 \cdot s \cdot Pa}) e^{-\frac{6,831K}{T_{Particle}}} \quad (2)$$

where the pre-exponential and the activation energy are derived from the paper by Lockwood et al. (1984) and the rate is zero below an onset temperature of 773 K. The devolatilization and char oxidation parameters are the same as those used in the validation study that is described later in this paper.

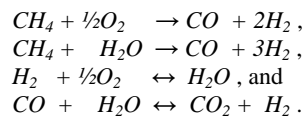
Gas-phase chemical reactions are accounted for using the slower of the mixing-limited and reaction-limited rates. For mixing-limited, the Eddy Dissipation Model (EDM) is used, with the rate given by

$$R_{EDM} = A_{EDM} \left(\frac{\varepsilon}{\kappa} \right) \min \left([\text{fuel}], \frac{[\text{oxidant}]}{C_{Stoich}} \right) \quad (3)$$

For reaction-limited, the finite rate chemistry (FRC) model is used, with the rate given by

$$R_{FRC} = A_{FRC} T^b e^{\left(\frac{-E_a}{RT} \right)} [\text{fuel}]^c [\text{oxidant}]^d \quad (4)$$

In the gas phase, there is one reaction accounting for the partial oxidation of coal volatiles, where $\text{volatiles} + 0.36O_2 \rightarrow 0.4CO + 0.56H_2O$. This reaction is assumed to be controlled by the rate of turbulent mixing and the EDM model is used with $A_{EDM}=1.5$. Methane oxidation is assumed to occur via the four reactions,



The rate is controlled by the slower of the EDM and FRC rates, where $A_{EDM}=4.0$ and A_{FRC} , E_a , b , c , and d are from the paper by Jones and Lindstedt (1988).

1.2 Coal Properties

The proximate and ultimate analyses of the James River Leatherwood coal are provided in Table 1. The volatile matter is assumed to have the physical properties of CH_4 for modelling purposes. In practice, moisture content is about 2% for coal injected into the blast furnace, so moisture evaporation from the coal was not included in the present model. The coal particle size distribution was measured and is provided in Figure 1. This distribution was implemented by tracking 28 distinct particle sizes. A total of 28,000 particles were tracked.

1.3 Geometry

A cut-away view of the model domain, showing the blowpipe, tuyere, and the two injection lances is provided in Figure 2. The blast air enters at the right (into the

blowpipe) and travels toward the left (out of the tuyere). The smaller diameter lance (NG lance) injects natural gas whose flow through the lance, including heat transfer with the blast air through the solid lance material, is included in this model. The larger diameter lance (PCI lance) has coal and air travelling through the centre tube and an annular cooling air flow surrounding it. The flow of coal and air through the centre tube is modelled, but the annular flow, which can be given a swirl, is specified as a boundary condition at the face of the lance as indicated in Figure 2. The grid for this computational domain consists of 1.15 million volumes.

Proximate Analysis (mass fraction)	
Ash	0.048
Volatiles	0.309
Moisture	0.170
Carbon (by difference)	0.473
Ultimate Analysis (mass fraction)	
Carbon	0.660
Hydrogen	0.044
Sulphur	0.007
Nitrogen	0.015
Chlorine	0.000
Oxygen (by difference)	0.056
(Ash & Moisture)	0.218

Table 1: Proximate and ultimate analyses of the James River Leatherwood coal used in the model.

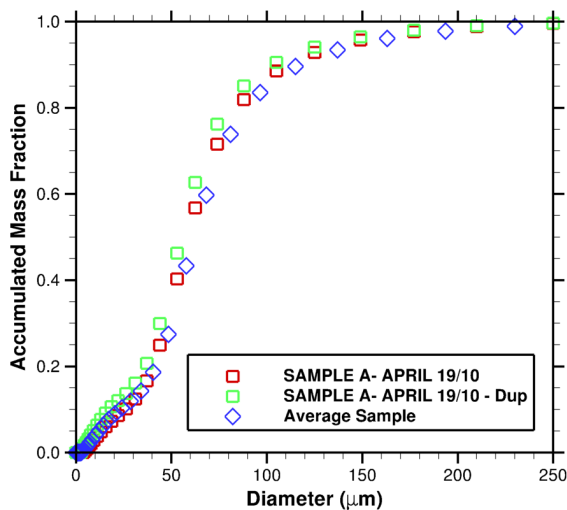


Figure 1: Coal particle size distribution. The “Average Sample” was used for the model.

1.4 Boundary Conditions and Properties

The inner surface of the tuyere has a temperature of 1172 K and an emissivity of 0.95. The blowpipe inner surface is adiabatic and has an emissivity of 0.95. The blast air has a temperature of 1372 K and flow rate of 2.99 kg/s. Enriched with oxygen, it consists of 28.5% O_2 by volume and 3% H_2O , with the balance being N_2 . The outlet at the end of the tuyere nozzle has an absolute pressure of 350 kPa and a radiation temperature, i.e., a hot black surface representing radiation from the raceway, of 2116 K.

The PCI lance inner surface, which is exposed to the coal/air flow, has a temperature of 311 K and an emissivity of 0.90. The outer surface of the PCI lance, which is exposed to the blast air, has a temperature of 1311 K and an emissivity of 0.90. The NG lance, which participates in heat transfer between the flows of blast air and natural gas, has an emissivity of 0.90 and a thermal conductivity of 14.2 W/(m·K).

The inlets of natural gas to the NG lance and of pulverized coal to the PCI lance are shown in Figure 3. The natural gas enters at a temperature of 311 K and its simplified composition consists of 97.7% CH_4 by volume and 0.685% CO_2 , with the balance being N_2 . The pulverized coal carrier is air with a temperature of 311 K and flow rate of 0.0689 kg/s. The coal has a temperature of 311 K and a flow rate of 0.296 kg/s. The annular cooling air flow in the PCI lance is varied in this study. In Case #1, it has zero flow and in Case #2 it has a temperature of 644 K and flow rate of 0.0528 kg/s. The swirl in Case #2 was determined from CFD simulations of the annular flow inside the lance in a previous study. The swirl vane angle is 9 degrees, which represents a low swirl case. Although there is swirling flow involved, the strength of the swirl is not particularly high so the standard $\kappa-\epsilon$ turbulence model, which is known to be inaccurate for strongly swirling flows, is expected to provide reasonable accuracy here.

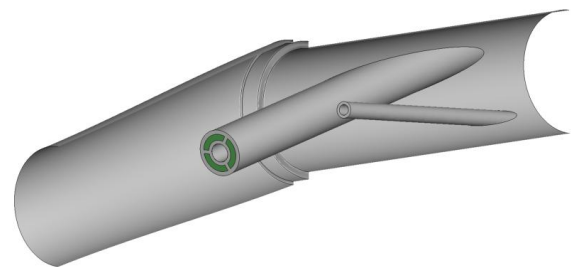


Figure 2: Cut-away view of the model domain: blowpipe, tuyere, natural gas lance, and pulverized coal lance with annular cooling flow (green).

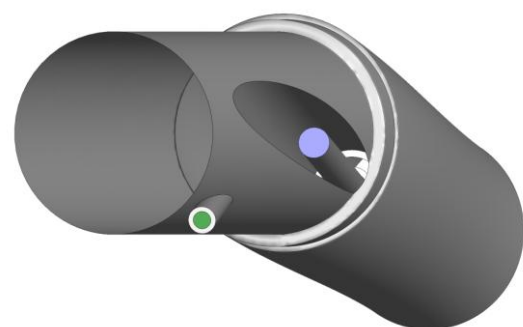


Figure 3: Inlets of natural gas (green) and pulverized coal (violet).

2. VALIDATION

Versions of this model have been used in the past on similar studies of commercial blast furnaces, so confidence has been developed over time in the overall approach.

Validation work was carried out and documented in the paper by Chui et al. (2003). That validation work is briefly described here.

Natural Resources Canada / CanmetENERGY developed a pilot plant facility that simulates blast furnace blowpipe-tuyere conditions. Its main component is a cylindrical reactor (1 m in length, 0.03 m internal diameter) consisting of a heavily insulated, refractory-lined inner core and a steel shell. Natural gas and coal were injected into this cylindrical reactor, and sampling ports, positioned 0.65 m downstream of the coal injection point, sampled O₂, CO₂, and CO.

The CFD model used by Chui et al. (2003) was identical to the model used in this work, except for the gaseous combustion model, which used a combination of the flamelet formulations for premixed and non-premixed combustion. According to the CO₂ and CO gas measurements, the CFD model predicted combustion reasonably well, only under-predicting the level of CO₂ and CO by 10-15%. The gaseous combustion model in the present work predicts a more rapid onset of combustion compared to the model used by Chui et al. (2003) so it would be expected to provide earlier heating of the coal, thereby trending the CO₂ and CO predictions closer to the measurements.

3. RESULTS

The overall observations with the annular cooling flow in the PCI lance turned off (Case #1) are reported here, as well as the effect of having the swirled annular cooling flow in the PCI lance turned on (Case #2).

3.1 Case#1 – Annular Cooling Flow Turned Off

The presence of the PCI lance and the natural gas injection cause a swirling motion of the blast air. This is apparent in Figure 4, which shows the gas temperature on several cutting planes across the tuyere. The hot products of natural gas combustion are swept downward as the flow passes around the PCI lance. This swirling of blast air caused by the presence of the lance is similar to the observation of Yeh et al. (2012).

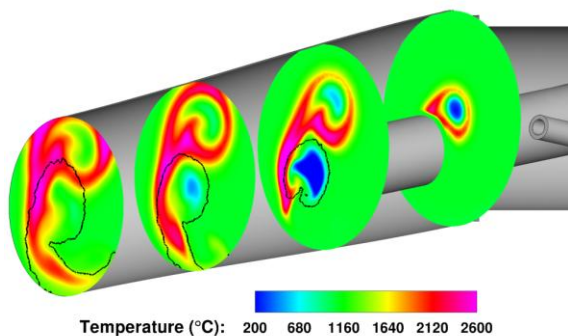


Figure 4: Gas temperature on cutting planes across the tuyere. The black outline on each plane denotes the extent of the coal particles.

Particle trajectories are found to depend on particle size. Figure 5 shows the trajectories of small, medium, and large particles. The smallest particles are drawn into the wake region of the PCI lance, which has created a bluff

body effect. This representation of the PCI lance is for Case #1, in which the swirling annular flow of cooling air is turned off, creating a recirculation zone at the face of the lance. Figure 5 also shows that the smallest particles are drawn into the downward swirling flow of blast air. The medium and large particles are less affected by the flow, having a more ballistic path, especially the largest particles. This behaviour is reflected in Figure 6, which shows the particle concentrations at the tuyere outlet.

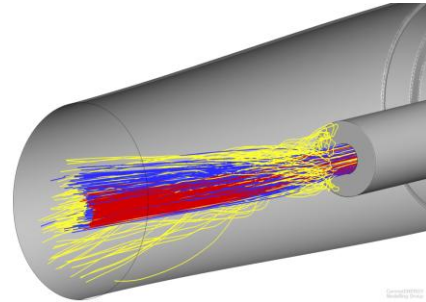


Figure 5: Particle trajectories for different particle sizes. Yellow: 3.0, 3.6 μm. Blue: 58, 68 μm. Red: 275, 325 μm.

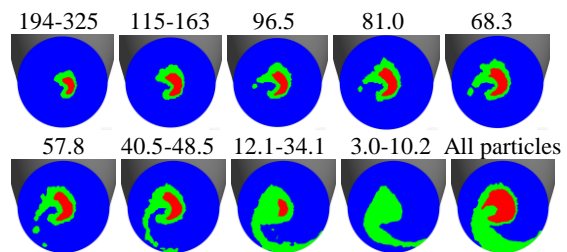


Figure 6: Particle volume fraction at tuyere outlet by group. Green $\geq 10^{-6} \text{ m}^3/\text{m}^3$. Red $\geq 10^{-4} \text{ m}^3/\text{m}^3$. The size (range) in μm is indicated above each plot.

Coal burnout is also found to depend on particle size. The burnout statistics are summarized in Figures 7 and 8. Devolatilization occurs for particles less than approximately 70 μm and char oxidation occurs for particles less than approximately 30 μm. Particles larger than approximately 100 μm exit the tuyere without any reaction. Unlike the finding of Yeh et al. (2012), the gaseous and solid fuels do not compete for oxygen because they are generally kept apart.

The swirling motion of the blast air flow is reflected in the distribution of heat flux to the tuyere, as illustrated in Figure 9. A high level of heat flux is found at the top. This is a consequence of the high-speed natural gas injection aimed in this direction. There is also a high level of heat flux at the bottom of the tuyere even though neither lance is pointed in this direction. This high heat flux is a consequence of the swirl imparted to the blast air by the lances and injection, sweeping the hot products of natural gas combustion, as well as small coal particles, downward.

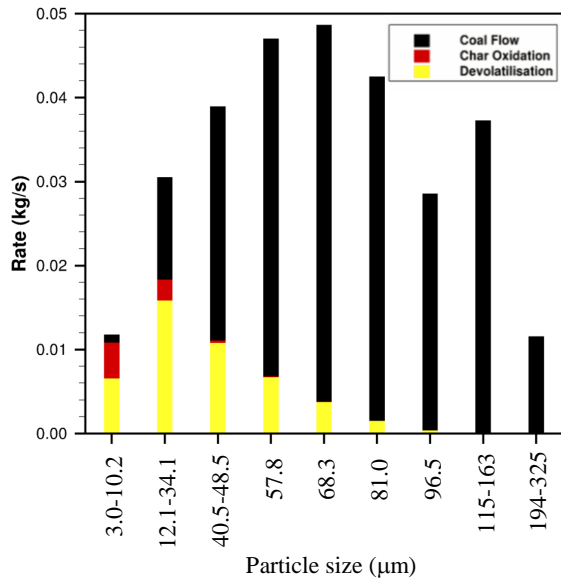


Figure 7: Coal flow rate versus particle size, showing the amount of devolatilization and char oxidation.

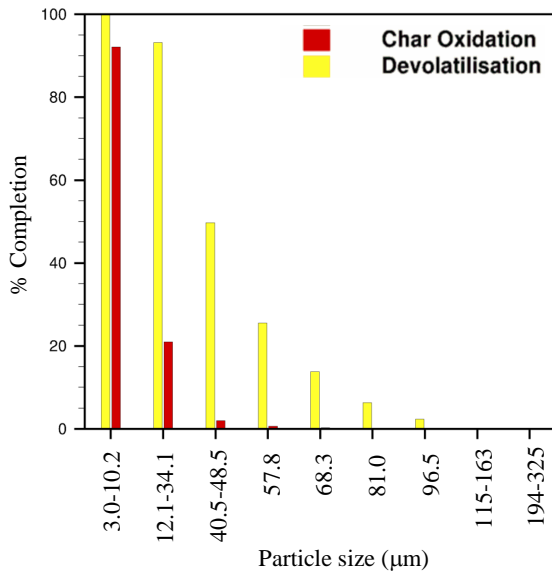


Figure 8: Percent completion versus particle size for devolatilization and char oxidation.

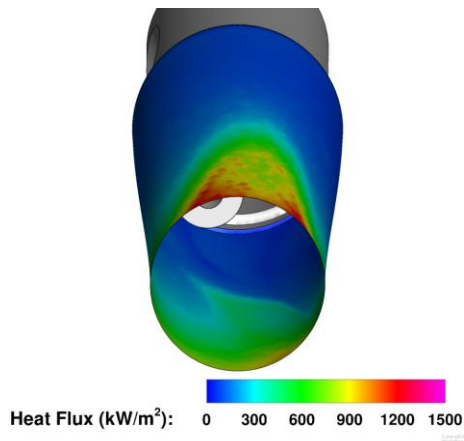


Figure 9: Heat flux to the tuyere.

3.2 Case #2 - Annular Cooling Flow Turned On

In Case #2, the annular cooling flow of the PCI injection lance is turned on. Its effect is examined by comparing the results to Case #1, in which there was no annular cooling flow. The comparison is provided in Figure 10. In the plot of Case #1, the coal appears to come from the entire face of the lance, but this is only because the smaller particles have been drawn into the recirculation zone at this face—the inner tube of the PCI lance is the same diameter in both cases. The effect of the swirling annular flow, surprisingly, is mainly to suppress the dispersion of coal relative to Case #1. This is because the bluff body effect that dispersed small coal particles no longer exists. In both cases, the effect of the swirl imparted to the blast air is apparent, although it is suppressed somewhat in Case #2.

The annular swirling flow from the PCI lance not only suppresses coal particle dispersion, but coal burnout as well. Figure 11 compares the burnout in Cases #1 and #2. In Case #2, both devolatilization and char combustion have been reduced.

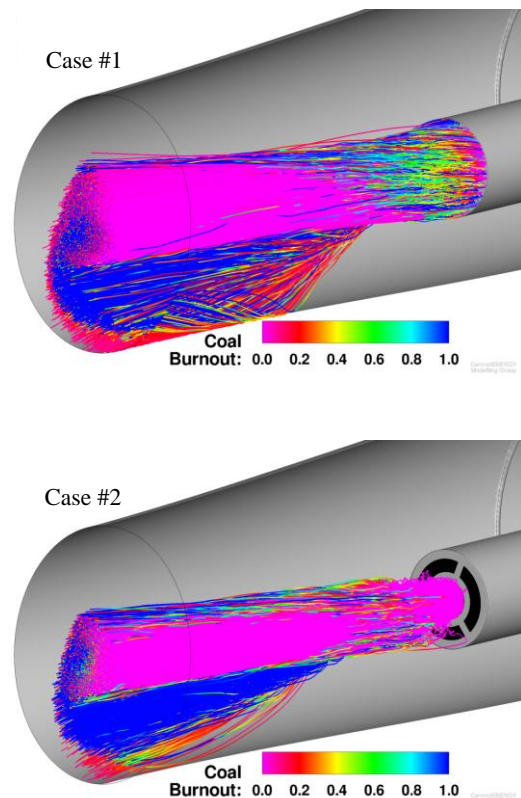


Figure 10: Coal particle tracks coloured by burnout for Cases #1 and #2.

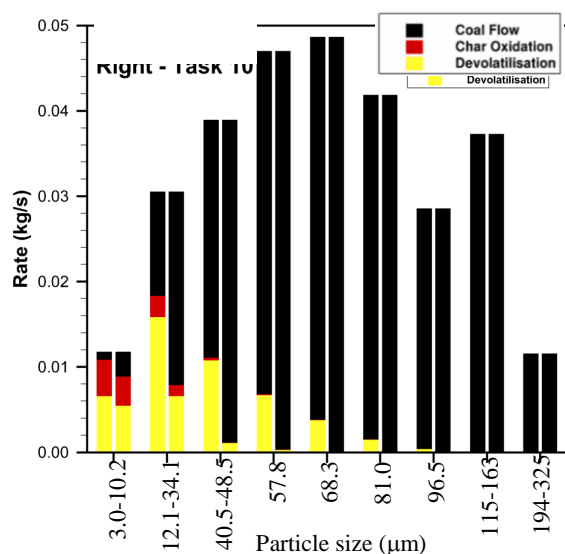


Figure 11: A comparison of devolatilization and char combustion for Cases #1 (left bar) and #2 (right bar).

CONCLUSION

This CFD study has focussed on the co-injection of pulverized coal and natural gas in blast furnaces for iron-making. It was found, unexpectedly, that the swirled annular cooling flow from the PCI lance actually suppressed the dispersion of coal particles and, consequently, suppressed burnout. Conversely, it was found that turning off the cooling air flow lead to a bluff body effect on the blast air, which enhanced coal dispersion, especially for the smaller particles. This implies that a swirling air jacket does not necessarily improve coal dispersion and that dispersion can be effected by a simpler lance configuration involving a bluff body effect. Based on these results, future studies will focus on a single lance that injects both coal and natural gas and employs the bluff body effect to enhance coal dispersion.

ACKNOWLEDGEMENT

This work was supported by the Program of Energy Research and Development of the Government of Canada.

REFERENCES

ANDHAZY, D., LOFFLER, G., WINTER, F., FEILMAYR, C., BURGLER, T., (2005), "Theoretical Analysis on the Injection of H₂, CO, CH₄ Rich Gases into the Blast Furnace", *ISIJ International*, **45**, 2, 166-174.

BADZIOCH, S., HAWKSLEY, P.G.W., (1970) "Kinetics of Thermal Decomposition of Pulverized Coal Particles", *Ind. Eng. Chem. Process Des. Develop.*, **9**, 4, 521-530.

CHUI, E.H., SCOTT, K.A., HARRISON, F.W., MACFADYEN, N.K., (2003), "MODELING THE CO-INJECTION OF COAL AND NATURAL GAS IN A HIGH SPEED ENVIRONMENT", *Seventh International Conference on Technologies and Combustion for a Clean Environment*, Lisbon, Portugal.

JAMALUDDIN, A.S., WALL, T.F., TRUELOVE, J.S., (1986), "COMBUSTION OF PULVERIZED COAL AS A TUYERE INJECTANT TO THE BLAST FURNACE", *Twenty-first Symposium (International) on Combustion / The Combustion Institute*, Munich, Federal Republic of Germany, 575-584.

JONES, W.P., LINDSTEDT, R.P., (1988), "Global Reaction Schemes for Hydrocarbon Combustion", *Combustion and Flame*, **73**, 233-249.

LOCKWOOD, F.C., RIZIVI, S.M.A., LEE, G.K., WHALEY, H., (1984), "Coal Combustion Model Validation Using Cylindrical Furnace Data", *Twentieth Symposium (International) on Combustion / The Combustion Institute*, Pittsburgh, USA, 513-522.

MATHIESON, J.G., TRUELOVE, J.S., ROGERS, H., (2005), "Toward an understanding of coal combustion in blast furnace tuyere injection", *Fuel*, **84**, 1229-1237.

NOGAMI, H., CHU, M., YAGI, J., (2005), "Multi-dimensional transient mathematical simulator of blast furnace process based on multi-fluid and kinetic theories", *Computers & Chemical Engineering*, **29**, 2438-2448.

SHEN, Y.S., GUO, B.Y., YU, A.B., ZULLI, P., (2009a), "A three-dimensional numerical study of the combustion of coal blends in blast furnace", *Fuel*, **88**, 255-263.

SHEN, Y.S., MALDONADO, D., GUO, B.Y., YU, A.B., AUSTIN, P., ZULLI, P., (2009b), "Computational Fluid Dynamics Study of Pulverized Coal Combustion in Blast Furnace Raceway", *Ind. Eng. Chem. Res.*, **48**, 10314-10323.

SHEN, Y.S., YU, A., AUSTIN, P., ZULLI, P., (2012), "Modelling in-furnace phenomena of pulverized coal injection in ironmaking blast furnace: Effect of coke bed porosities", *Minerals Engineering*, **33**, 54-65.

YEH, C.P., DU, S.W., TSAI, C.H., YANG, R.J., (2012), "Numerical analysis of flow and combustion behavior in tuyere and raceway of blast furnace fueled with pulverized coal and recycled top gas", *Energy*, **42**, 233-240.